

# Preparation of Polyurethane Nanofibers by Electrospinning

Haitao Zhuo, Jinlian Hu, Shaojun Chen, Lapyan Yeung

*Institute of Textiles and Clothing, Hong Kong Polytechnic University, Hung Hom, Kowloon, Hong Kong, China*

Received 20 June 2007; accepted 10 January 2008

DOI 10.1002/app.28067

Published online 28 March 2008 in Wiley InterScience (www.interscience.wiley.com).

**ABSTRACT:** Polyurethane (PU) nanofibers were prepared by the electrospinning method. The process parameters, including the applied voltage, feeding rate, and solution concentration, were investigated carefully. The results showed that the resultant nanofibers, electrospun from PU/*N,N*-dimethylformamide (DMF) solutions, had ultrafine diameters ranging from about 700 to 50 nm. In addition, it was found that the diameters and morphology of the nanofibers were influenced greatly by the process parameters. In particular, the solution concentration played a main role in influencing

the transformation of the polymer solution into ultrafine fibers, and the diameters increased with the solution concentrations increasing. Finally, it was concluded that uniform PU nanofibers without beads or curls could be prepared by electrospinning through good control of the process parameters, such as 5.0–7.0 wt % PU/DMF solutions, 10–15-kV applied voltages, and 0.06–0.08 mm/min feeding rates. © 2008 Wiley Periodicals, Inc. *J Appl Polym Sci* 109: 406–411, 2008

**Key words:** films; nanotechnology; polyurethanes

## INTRODUCTION

Fibers with oriented polymer chains and diameters of 100 nm or less (nanofibers) are of great interest in science and technology.<sup>1</sup> One of the preparation methods for ultrafine fibers is electrospinning. It is a process that produces continuous polymer fibers with ultrafine diameters through the action of an external electric field imposed on a polymer solution or melt.<sup>2,3</sup> Because of their large surface area to volume ratio and the unique nanometer-scale architecture built by nanofibers, great potential applications are being explored in many fields, such as tissue engineering scaffolds, drug delivery media, filtration media, and protective clothes.<sup>4,5</sup> In principle, after the molecular parameters and process parameters are provided, nearly all soluble or fusible polymers can be processed into nanofibers by electrospinning,<sup>6</sup> including biopolymers or modified biopolymers such as collagen and chitosan, water-soluble polymers such as poly(ethylene oxide) and poly(vinyl acetate), bioerodible polymers such as polylactide and poly( $\epsilon$ -caprolactone), organosoluble polymers such as polyurethanes (PUs) and polystyrene, and melt-electrospun polymers such as polyethylene and polypropylene.

In particular, among PUs, there is one group of very promising smart materials called shape-memory polyurethanes (SMPUs). They can change their shape, hydroabsorbency, water vapor permeability, self-cleaning ability, and optical and other properties when external stimuli change.<sup>7,8</sup> Their shape-memory effects, including shape fixity and shape recovery, are influenced by many factors, such as the soft-segment length, hard-segment content, and thermomechanical conditions.<sup>9,10</sup> Generally, the soft-segment phase and hard-segment domains play the roles of the reversible phase and fixed phase in the shape-memory effect, respectively.<sup>9</sup> In addition, it has been proved that the high crystallinity of the soft segment at room temperature and the formation of stable hard-segment domains acting as physical crosslink points in the temperature range above the melting temperature of the soft-segment crystal are the two necessary conditions for segmented PU exhibiting a shape-memory effect.<sup>11</sup> So far, SMPUs have been widely researched by material scientists.<sup>12–16</sup> However, the research of SMPUs still stops at the millimeter scale. Many unique properties have not been explored, especially those on the nanometer scale.

Another application of SMPUs in textiles is strongly dependent on the manufacture of shape-memory fibers. Traditional methods of preparing polymer fibers include melt spinning, spinning from a solution or liquid-crystalline state, and forming fibers from a gel state.<sup>17–19</sup> Recently, SMPU fibers have been achieved by wet spinning and melt spinning,<sup>20,21</sup> but there are few related reports on electro-

Correspondence to: J. Hu (tchujl@inet.polyu.edu.hk).

Contract grant sponsor: Hong Kong Innovation Technology Funding (through the "High Performance Advanced Materials for Textiles and Apparels" project).

spinning. It is therefore necessary to develop this novel technology to prepare SMPU nanofibers. They are expected to be very novel and smart materials having many unique properties.

Before the unique properties of SMPU on a nanometer scale can be investigated, good PU nanofibers are expected to be prepared. Therefore, in this work, the electrospinning method was used to spin PU nanofibers, and conditional experiments were conducted to evaluate the effects of various parameters on the diameters and morphology of PU nanofibers, such as the applied voltage, feeding rate, and solution concentration.

## EXPERIMENTAL

### Materials

Poly( $\epsilon$ -caprolactone) diol (PCL; Daicel Chemical Industries, Ltd., Tokyo, Japan), with a number-average molecular weight of 4000 g/mol, was dried and degassed at 80°C under 0.1–0.2 kPa for 12 h before PU synthesis. *N,N*-Dimethylformamide (DMF; Aldrich, Auckland, New Zealand) and 1,4-butanediol (BDO; Acros, St. Louis, MO) were dried with 4-Å molecular sieves for several days before use. Extrapure-grade 4,4'-methylene diphenyl diisocyanate (MDI; Aldrich) was used directly.

### Synthesis of PU

PU resin (number-average molecular weight = 180,000 g/mol), based on PCL containing a 75% soft-segment content and 4000 soft-segment length, was synthesized by the bulk polymerization method. The reaction to prepare the prepolymer was carried out in a 500-mL conical flask equipped with a mechanical stirrer. First, PCL was mixed with MDI, and this was followed by chain extension with BDO for 30 min at the ambient temperature. After they were mixed evenly, the resulting prepolymer was poured from the flask into a Teflon pan, and a postcuring process was carried out in a vacuum oven at 80°C. After 10 h, the bulk-polymerized thermoplastic PU resin was obtained.<sup>22,23</sup>

### Preparation of the PU solution/PU bulk film

In this experiment, the PU/DMF solution for electrospinning was obtained after the PU resin was dissolved in DMF at the ambient temperature. For the investigation of the concentration influence, the original polymer solution was diluted with DMF into several new solutions with concentrations of 3.0, 5.0, 7.0, 10.0, and 12.0 wt %. At the same time, the PU bulk film was obtained after DMF had evaporated completely from the PU/DMF solution on the Teflon pan at 80°C in the oven.

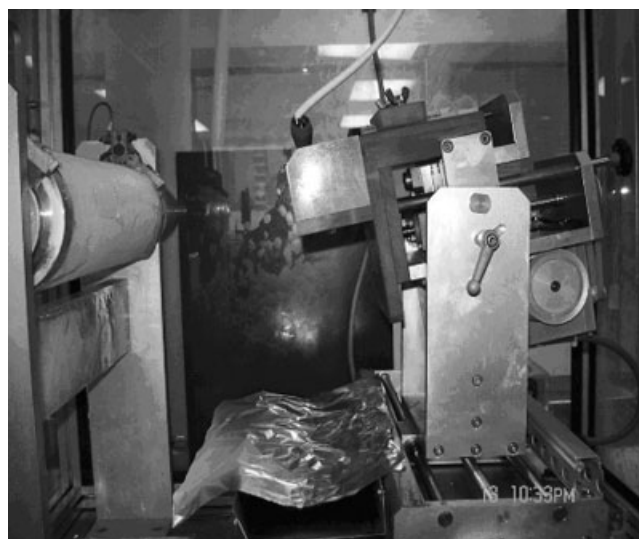


Figure 1 Electrospinning apparatus.

### Electrospinning

The electrospinning technique, described extensively in the literature,<sup>1–5</sup> involves applying an electric field to a polymeric solution to produce micrometer-to-nanometer fibers. The shape and surface morphology of the fibers depend on the electrospinning parameters used. The electrospinning process itself involves applying a high voltage to the tip of a syringe needle. Its schematic diagram has been described in detail in the literature.<sup>24</sup>

The electrospinning apparatus, as shown in Figure 1, consisted of a 5-mL syringe connected to a syringe pump. The solution flow rates were controlled by a syringe pump and ranged from 0.04 to 0.10 mm/min. The applied positive voltage was in the range of 12–25 kV. The target for the electrospun fibers was placed 15 cm from the needle tip and consisted of grounded aluminum. The electrospinning process was carried out at the ambient temperature.

### Characterization

Scanning electron microscopy (SEM; model S450, Hitachi, Tokyo, Japan) was used to investigate the morphology of the samples. Samples for SEM were obtained by the direct spinning of the nanofibers onto aluminum foil. The nanofibers were dried over a period of 2 days at the ambient temperature. The samples were gold-coated before SEM.

Differential scanning calorimetry (DSC) testing was performed with a PerkinElmer DSC machine (Waltham, MA). The samples (ca. 5 mg) were heated from –60 to 250°C at a heating rate of 10°C/min; then they were kept at a constant temperature of 250°C for 2 min and subsequently cooled to –60°C at the same rate. Finally, the first heating scan was

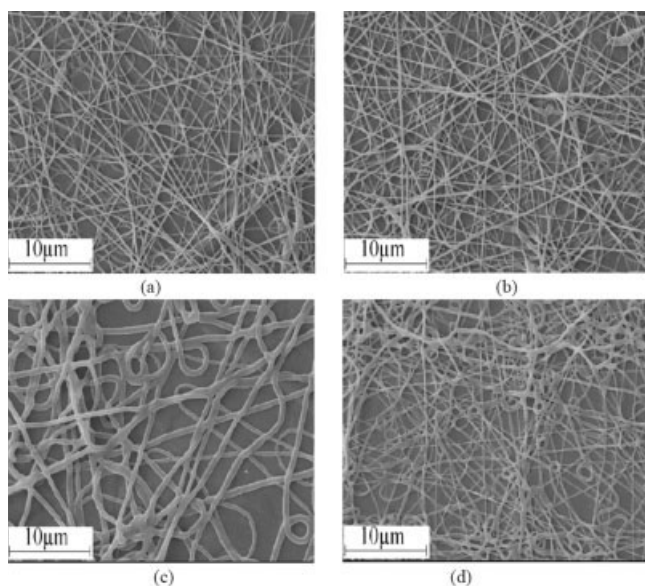


**Figure 2** SEM images of the nanofibers at different applied voltages: (a) 12, (b) 15, (c) 20, and (d) 25 kV.

repeated. The result from the second heating scan of each sample was used as a reference.

## RESULTS AND DISCUSSION

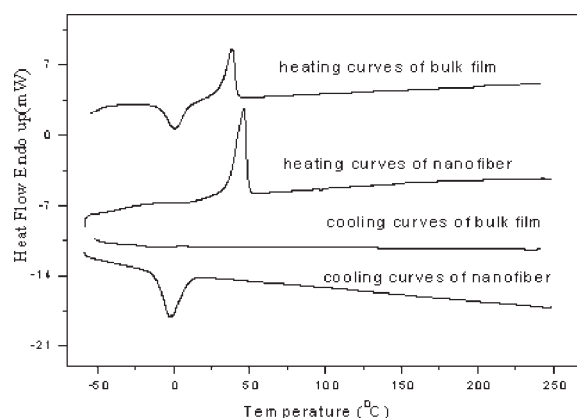
### Influence of the applied voltage

Figure 2 shows the SEM images of the resultant nanofiber samples spun from the 5.0 wt % PU/DMF solution at various applied voltages. In this study, it was found that uniform nanofibers without beads could not be obtained until the applied voltage reached 12.0 kV. If the applied voltage was not high enough (e.g., 10.0 kV), the PU solution could not be spun into nanofibers because of the lower electrical force. That is, 12.0 kV was a critical value for preparing uniform PU nanofibers with 5.0 wt % PU/DMF solutions. However, when the applied voltages were increased to a high value, such as 20.0 or 25.0 kV, the diameters of nanofibers appeared to be not uniform, and many loops formed in the resultant samples [Fig. 2(c,d)]. Generally, these results are ascribed to the excessively increased voltage. When the applied voltage is beyond a critical value, the higher electrical force will break the ideal balloon, and the jet also will not be stable during the electrospinning process.<sup>25</sup>

Figure 3 shows DSC curves of the nanofiber-deposited membrane and its bulk film. There were noticeable differences between the two samples, even though they had the same composition. For instance, the recrystallization peak appeared on the cooling curve for the nanofibers, whereas it appeared on the heating curves for the bulk film. This indicated that higher tropism was formed in the nanofibers, and

they were easier to recrystallize during the cooling process. Accordingly, the crystal of the soft segment in the nanofibers would be more stable during the heating process. As expected, the soft-segment melting temperature (ca. 46.34°C) of the nanofibers was much higher than that of the bulk film (ca. 38.53°C; shown in Fig. 3), and the enthalpy value of the nanofibers (ca. 40.85 J/g) was also much higher than that of the bulk film (ca. 22.30 J/g). These results indicated that the crystallization degree in the nanofibers was much higher than that in the bulk film. In addition, an evident glass transition appeared on the heating curves for the nanofiber samples, whereas it is not easy to distinguish the glass transition in the bulk film samples because of their lower heat capacity change. This implied that the microphase separation in the morphology of the nanofiber-deposited membrane was insufficient in comparison with the bulk PU film. The reason is that the nanofiber-deposited membrane was spun directly at the ambient temperature without an additional annealing process, whereas the bulk film was put in the 80°C oven for 24 h in this experiment. Therefore, a good microphase-separation morphology was more easily formed in the bulk film, and its lower heat capacity change during the glass transition could not be tested easily by DSC. Most importantly, from the DSC curves, it was found that the nanofiber-deposited membrane and bulk film both had a crystalline soft-segment phase. As mentioned previously, this structure satisfied the requirements of SMPU.<sup>9,22</sup> Moreover, the shape-memory behaviors of the PU bulk film were demonstrated in the earlier report.<sup>22,23</sup> Thus, this observation implied that PU was expected to keep its original morphology, although it had been spun into ultrafine fibers, that is, PU nanofibers.

In addition, as shown in Table I, the melting temperature of the soft segment in the nanofiber membrane increased with the applied voltage increasing,



**Figure 3** DSC curves of the resulting nanofiber-deposited membrane and the bulk film.

**TABLE I**  
**Electrospinning Parameters and Thermal Properties of the As-Spun Nanofibers**

Sample	Applied voltage (kV)	Concentration (wt %)	$T_m$ (°C)	$T_c$ (°C)
N1	12	3	42.11	—
N2	12	5	40.95	—
N3	12	7	40.63	—
N4	12	12	40.31	-1.19
N5	12	5	40.71	-2.12
N6	15	5	41.04	-0.96
N7	20	5	41.08	1.39
N8	25	5	43.06	3.98

$T_m$  = melting temperature of the soft segment;  $T_c$  = recrystallization temperature of the soft segment.

ranging from 40.4 to 43.2°C on the heating scans, and the recrystallization temperature also increased with increasing applied voltage on the cooling scans. This indicated that the PU nanofibers were easier to crystallize during the cooling process when the applied voltage was high because the higher electrical force resulted in better tropism in the molecular chain. This was another proof that the chain tropism in the nanofibers increased with the applied voltage increasing. More stable crystals could be formed in the nanofiber soft-segment phase.

### Influence of the feeding rate

As reported earlier,<sup>26</sup> the feeding rate affects the volume charge density and electrical current of a polymer solution. The electrical current increases with the feeding rate increasing in certain polymer solutions, whereas it decreases with the feeding rate increasing in other polymer solutions. For instance, it was observed by Theron et al.<sup>27</sup> that an increased feeding flow rate would increase the electrical current in poly(ethylene oxide), poly(vinyl acetate), poly(acrylic acid), and PU solutions, whereas it reduced the electrical current in PCL solutions. Thus, increasing the feeding flow rate would decrease the fiber diameter, and the surface charge density would decrease as the flow rate increases.<sup>26–28</sup> It was also pointed out by Zong et al.<sup>29</sup> that a different morphology could be achieved by control of the feeding rate at a given electric field because a certain minimum value of the solution volume suspended at the end of the spinneret should be maintained to form an equilibrium Taylor cone. Besides, Um et al.<sup>30</sup> demonstrated that with the feeding rate of the polymer solution increasing, the electrospinning performance for creating nanofibers improved; however, the improvement was not sufficient to achieve a consistent production of high-quality nanofiber membranes.

With reference to these studies, in this study, different feeding rates were used to investigate the

effect of the feeding rate on the morphology of the nanofibers. Figure 4 shows the SEM images of electrospun fibers spun at different feeding rates. The larger diameter nanofibers were spun at a higher feeding rate (e.g., 0.1 mm/min), and smaller and uniform nanofibers were observed in the samples spun at a lower feeding rate (e.g., 0.06 mm/min). This result was quite different from the previous observation by Theron and coworkers,<sup>27,28</sup> but it was confirmed by Kim et al.<sup>31</sup> This happened because the droplet suspended at the end of the spinneret at the higher feeding rate was larger than that at the lower feeding rate.<sup>17,21</sup> That is, its solution jet could carry a larger quantity of fluid; under the same applied voltage, the electrical force was equal, and it stretched the same-length nanofibers. However, they were harder to dry before they reached the collecting screen. Consequently, nonuniform and larger diameter nanofibers were formed in the final morphology because of the higher feeding rate [see Fig. 4(c,d)]. Knowing that the nanofiber performance could be improved, we could electrospin uniform nanofibers at a lower feed rate (e.g., 0.06 or 0.08 mm/min).

### Influence of the concentration

Five PU/DMF solutions with different concentrations (3.0, 5.0, 7.0, 10.0, and 12.0 wt %) were used to spin PU nanofibers. During the experimental process, jet formation was not observed in the PU/DMF solutions above 12.0 wt % because of their higher viscosity, whereas in a too diluted solution (e.g., <3.0 wt %), the jet broke into droplets; electrospraying instead of electrospinning was observed. This

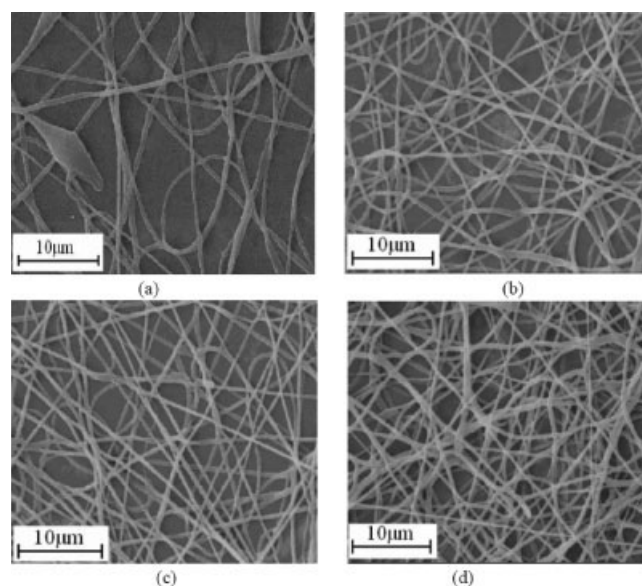


**Figure 4** SEM images of the nanofibers at different feeding rates: (a) 0.04, (b) 0.06, (c) 0.08, and (d) 0.1 mm/min.

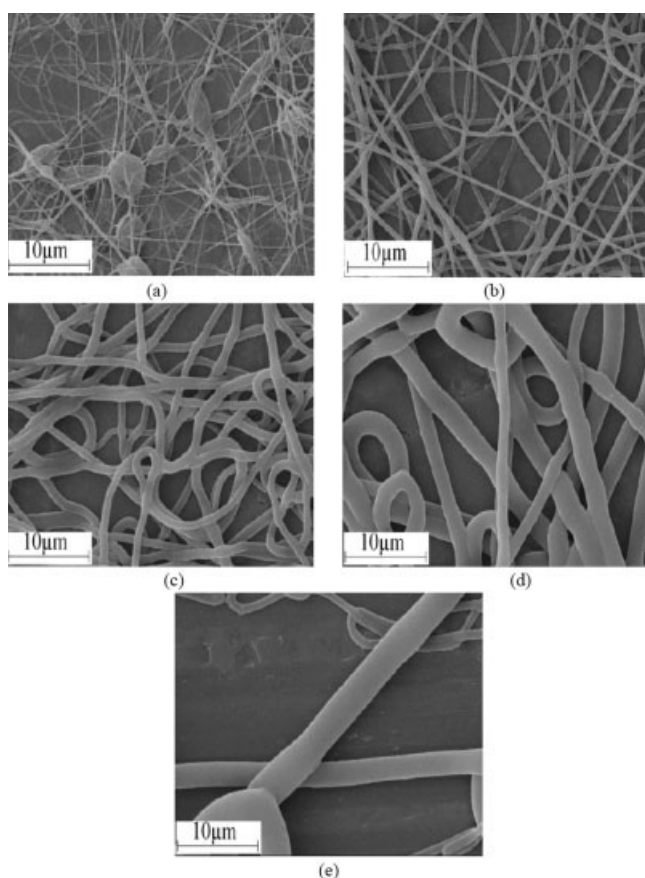


**Figure 5** SEM images showing nanofibers spun from different concentrations: (a) 3.0, (b) 5.0, (c) 7.0, (d) 10.0, and (e) 12.0 wt %.

means that continuous nanofibers also cannot be prepared if the viscosity is too low. This is because higher electrical forces are required to overcome both the surface tension and the viscoelastic force for stretching into fibers as the concentration or, equivalently, the viscosity increases. Thus, the concentrations of 3.0 and 12.0 wt % were called the lower and upper crucial concentrations for electrospinning a PU/DMF solution into nanofibers, respectively, in this system.

SEM images of electrospun nanofibers spun with solutions of different concentrations are presented in Figure 5. They show a significant difference in the diameter and morphology of the nanofibers. As previously discussed, it was very difficult to spin a continuous fiber at a concentration below 3.0 wt %. Even though the solution could be successfully spun into nanofibers, the resultant nanofibers were usually not uniform because of its too low surface tension and viscoelastic force. Thus, it was observed that a mixture of beads (or drops) with nanofibers were prepared [Fig. 5(a)]. In contrast, with too high concentrations (e.g., >10.0 wt %), nanofibers were also harder to dry well because of their high surface tension before they reached the collecting screen. Then,

the resultant nanofibers usually combined with another, as shown in Figure 5(d,e).

In addition, the diameters of the nanofibers were also quite different. For example, 50–100-nm nanofibers were prepared from a 3.0 wt % solution, and 600–700-nm nanofibers were observed in the 12.0 wt % spun samples (shown in Fig. 5). In fact, the diameters increased linearly with the concentration increasing. In this way, nanofibers with different diameters can be easily prepared by control of the concentration solution. At the same time, from the thermal properties of the nanofiber-deposited membranes, it could be found that the melting temperature decreased when the polymer solution concentration increased (shown in Table I). This result also could be ascribed to the microphase-separation structure of the nanofibers. The higher concentration resulted in less microphase-separation structure in comparison with the low concentration because it was harder to dry during the electrospinning process.

## CONCLUSIONS

In this experiment, PU nanofibers were successfully prepared from PU/DMF solutions by the electrospinning method; the applied voltage, feeding rate, and solution concentration influenced the diameters and morphology greatly. The following conclusions could be drawn:

1. In this system, the best nanofibers could be electrospun from a 5.0 wt % solution concentration with a 12.0-kV applied voltage and 0.08 mm/min feeding rate after the distance between the capillary tip and grounded collector was controlled, and the diameter, ranging from 50 to 700 nm, could be changed by adjustments of the electrospinning parameters.
2. The DSC results indicated that the resultant nanofibers showed a morphology similar to that of the bulk film that could satisfy the structure requirements of PU having a shape-memory effect.
3. A low applied voltage results in more uniform nanofibers, and the largest diameter fibers were formed at the higher solution feeding rates. The solution concentration played a main role in affecting the diameter and morphology; the nanofiber diameters increased with the concentration linearly.

## References

1. Bergshoef, M. M.; Vancso, G. J. *Adv Mater* 1999, 11, 1362.
2. Demir, M. M.; Yilgor, I.; Yilgor, E. *Polymer* 2002, 43, 3303.
3. Casper, C. L.; Stephens, J. S.; Tassi, N. G.; Chase, D. B.; Rabolt, J. F. *Macromolecules* 2004, 37, 573.

4. Inai, R.; Kotaki, M.; Ramakrishna, S. *Nanotechnology* 2005, 16, 208.
5. Huang, Z. M.; Zhang, Y. Z.; Kotaki, M.; Ramakrishna, S. *Compos Sci Technol* 2003, 63, 2223.
6. Greiner, A.; Wendorff, J. H. *Angew Chem Int Ed* 2007, 46, 5670.
7. Lee, B. S.; Chun, B. C.; Chung, Y. C.; Sul, K., II; Cho, J. W. *Macromolecules* 2001, 34, 6431.
8. Choi, N. Y.; Kelch, S.; Lendlein, A. *Adv Eng Mater* 2006, 8, 439.
9. Kim, B. K.; Lee, S. Y.; Xu, M. *Polymer* 1996, 37, 5781.
10. Hu, J. L.; Ji, F. L.; Wong, Y. W. *Polym Int* 2005, 54, 600.
11. Li, F. K.; Zhang, X.; Hou, J. N.; Xu, M.; Luo, X. L.; Ma, D. Z.; Kim, B. K. *J Appl Polym Sci* 1997, 64, 1511.
12. Chen, S. J.; Cao, Q.; Liu, P. S. *Acta Polym Sin* 2006, 1, 1.
13. Lin, J. R.; Chen, L. W. *J Appl Polym Sci* 1998, 69, 1575.
14. Chen, S. J.; Cao, Q.; Jing, B.; Cai, Y. L.; Liu, P. S.; Hu, J. L. *J Appl Polym Sci* 2006, 102, 5224.
15. Hu, J. L.; Yang, Z. H.; Yeung, L. Y.; Ji, F. L.; Liu, Y. Q. *Polym Int* 2005, 54, 854.
16. Zhu, Y.; Hu, J. L.; Yeung, K. W.; Fan, H. J.; Liu, Y. Q. *Chin J Polym Sci* 2006, 24, 173.
17. Dees, J. R.; Spruiell, J. E. *J Appl Polym Sci* 1974, 18, 1053.
18. Barham, P.; Keller, J. *J Mater Sci* 1985, 20, 2281.
19. Deitzel, J. M.; Kleinmeyer, J.; Harris, D.; Becktan, N. C. *Polymer* 2001, 42, 261.
20. Hu, J. L.; Fan, H. J.; Ye, G. D.; Liu, Y.; Yang, G. L. *Chin. Pat. CN200410049347.1* (2004).
21. Hu, J. L.; Yang, Z. H.; Yang, G. L.; Huang, Y. H. *Chin. Pat. CN200410049303.9* (2004).
22. Chen, S. J.; Hu, J. L.; Liu, Y. Q.; Liem, H. M.; Zhu, Y.; Liu, Y. J. *J Polym Sci Part B: Polym Phys* 2007, 45, 444.
23. Chen, S. J.; Hu, J. L.; Liu, Y. Q.; Liem, H. M.; Zhu, Y.; Meng, Q. H. *Polym Int* 2007, 56, 1128.
24. Son, W. K.; Youk, J. H.; Lee, T. S. *Polymer* 2004, 45, 2959.
25. Lee, J. S.; Choi, K. H.; Ghim, H. D. *J Appl Polym Sci* 2004, 93, 1638.
26. Nasir, M.; Matsumoto, H.; Danno, T.; Minagawa, M.; Irisawa, T.; Shioya, M.; Tanioka, A. *J Polym Sci Part B: Polym Phys* 2006, 44, 779.
27. Theron, S. A.; Zussman, E.; Yarin, A. L. *Polymer* 2004, 45, 2017.
28. Reznok, S. N.; Yarin, A. L.; Theron, A. L.; Zussman, E. *J Fluid Mech* 2004, 516, 349.
29. Zong, X. H.; Kim, K. S.; Fang, D. F.; Ran, S. F.; Hsiao, B. S.; Chu, B. *Polymer* 2002, 43, 4403.
30. Um, I. C.; Fang, D. F.; Hsiao, B. S.; Okamoto, A.; Chu, B. *Bio-macromolecules* 2004, 5, 1428.
31. Kim, S. J.; Lim, J. Y.; Kim, I. Y. *Smart Mater Struct* 2005, 14, N16.